SUPPLEMENTARY INFORMATION

Sensitive Detection and Tracking of Spontaneous Metastases in Deep Tissues via a Genetically Encoded Magnetic Resonance Imaging Reporter

Nivin N. Nyström[1,2], Sean W. McRae[1,3], Francisco M. Martinez[3], John J. Kelly[3], Timothy J. Scholl[1,3,4,5,#], John A. Ronald[*,1,3,6,#]

[1]Department of Medical Biophysics, Western University, London, ON, Canada
[2]Department of Chemical Engineering, California Institute of Technology, Pasadena, CA, USA
[3]Imaging Laboratories, Robarts Research Institute, Western University, London, ON, Canada
[4]Department of Physics and Astronomy, Western University, London, ON, Canada
[5]Ontario Institute for Cancer Research, Toronto, ON, Canada
[6]Lawson Health Research Institute, London, ON, Canada

[#]These are co-senior authors.
*Correspondence can be addressed to T.J.S. (tscholl@robarts.ca) and J.A.R. (jronald@robarts.ca).

Reference	Genetic Construct	Field	Gd(III) Dose	Performance
Patrick et al. *PNAS* (2014)	Doxycycline-inducible Oatp1a1 lentivirus transfer plasmid	7T, 9.4T	0.664 to 2 mmol/kg	7.8-fold greater signals than control xenograft at highest dose of 2 mmol/kg
Wu et al. *FASEB* (2018)	Constitutively expressed Oatp1b3 lentivirus transfer plasmid	7T	~2 mmol/kg*	2.7-fold greater signals than control xenografts
Nyström et al. *Invest Radiol* (2019)	Constitutively expressed Oatp1a1 lentivirus transfer plasmid	3T	0.1 mmol/kg	2.6-fold greater signals than control tumors
Kelly et al. *Sci Adv* (2021)	Constitutively expressed Oatp1a1 CRISPR-Cas9 knock-in	3T	1.67 mmol/kg	2.9-fold greater signals than control xenografts

Table S1. Summary of *Oatp1*-MRI *in vivo* imaging publications, with information on genetic construct design, field strength, and Gd-EOB-DTPA dose. *Calculated from a reported administration of 200 µl of 250 mM Gd-EOB-DTPA per mouse, assuming an average weight of 25 g per mouse.

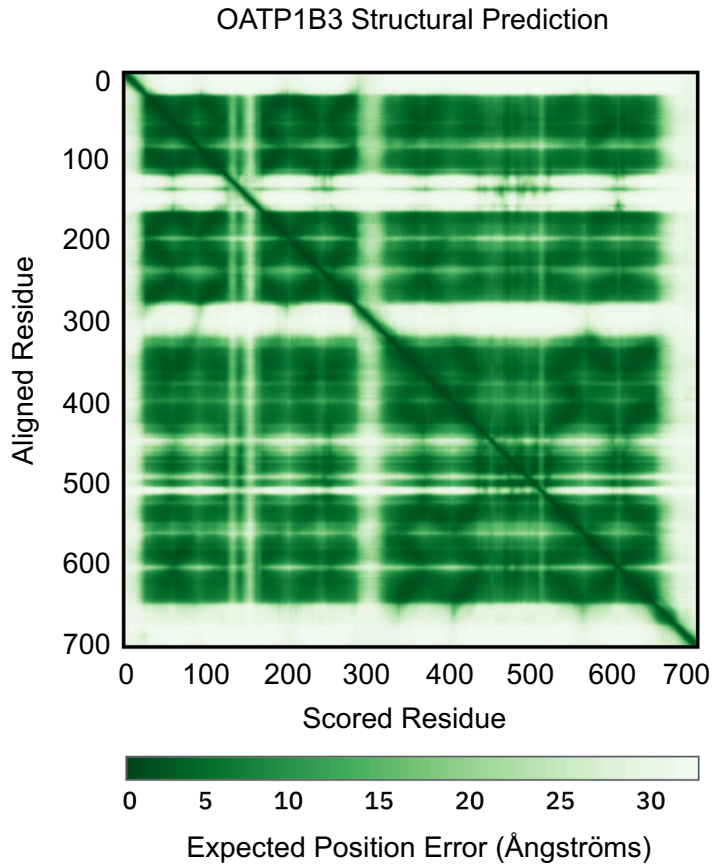

Figure S1. Predicted aligned error plot for OATP1B3, where expected position error for the aligned residue is assigned an expected position error (Ångströms) against the rest of the protein sequence. The transmembrane domains of OATP1B3 exhibit low expected position error (<5 Å) whereas high expected position error (>25 Å) is demonstrated at both termini, Extracellular Domain 2 (ECD2) and Cytoplasmic Domain 4 (CD4).

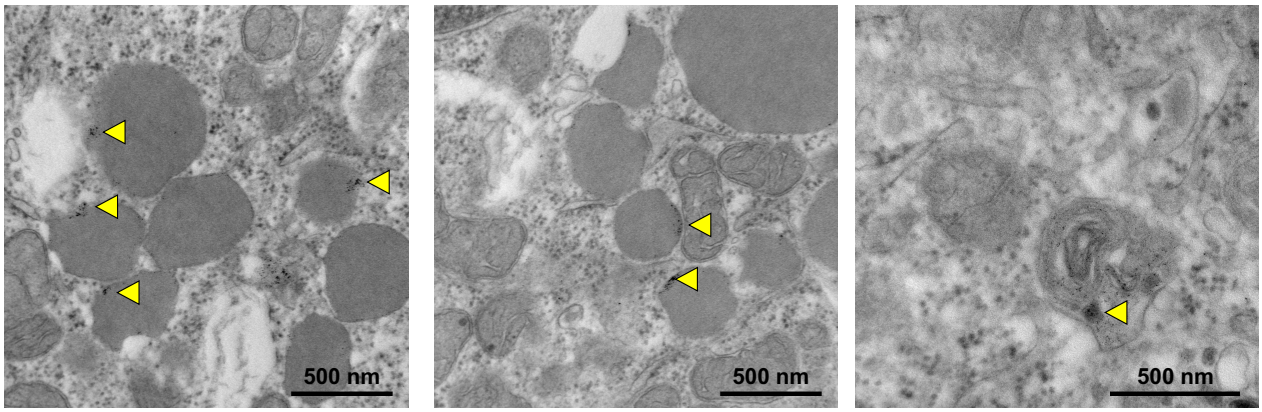

Figure S2. Transmission electron microscopy of Luc-1B3 cells incubated with 1 mM Gd-EOB-DTPA (appearing as black foci in TEM images, highlighted by yellow arrows) for 1 hour. Gd(III) is shown to be encapsulated in residual bodies, which are typically destined for exocytosis. Scale bar, 500 nm.

Glycosylation Sites	Phosphorylation Sites	Disulfide Bonds	Kazal 1-like Domain
134	293	459 ↔ 489	453-508*
145	295	465 ↔ 485	
151	683	474 ↔ 506	
445			
503			
516			

Table S2. Predicted post-translational regulatory positions of OATP1B3. N-linked glycosylation to asparagine residues, which has been correlated to promotion of transporter function (31). Phosphorylation of serine residues has been correlated to downregulation of transporter activity (29). Disulfide bonds within the Kazal-1 like domain are predicted to result in serine protease inhibitor activity.

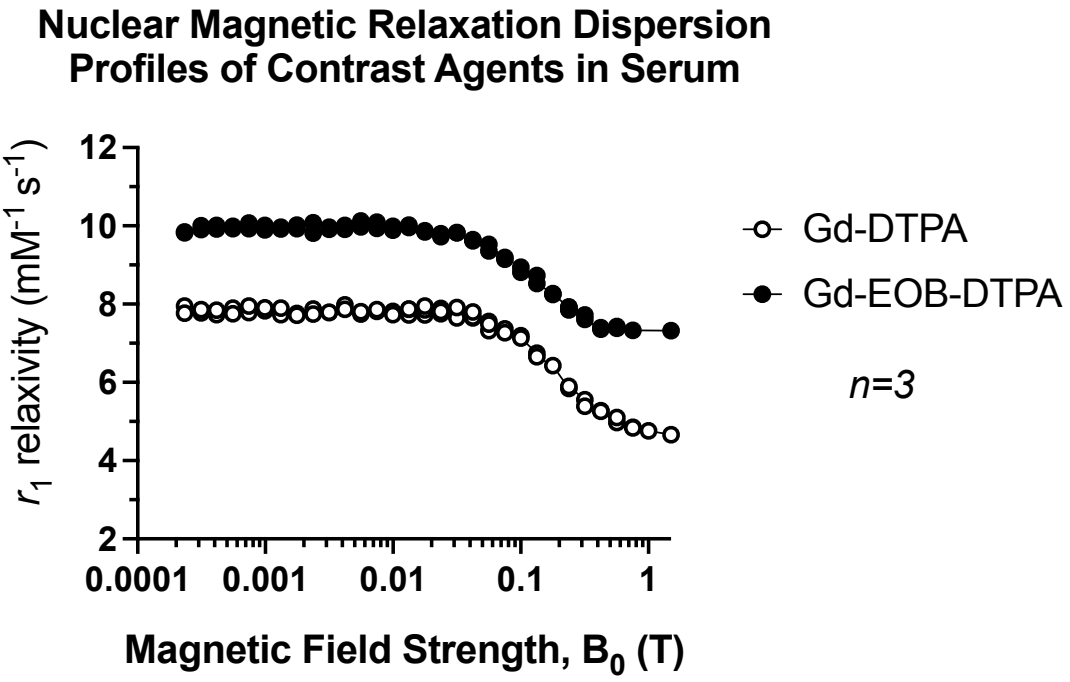

Figure S3. Nuclear magnetic relaxation dispersion (NMRD) profiles of Gd-DTPA and Gd-EOB-DTPA measured at 37ºC. NMRD data for fields <1 T were acquired using a fast field-cycling relaxometer and extended by an inversion-recovery measurement at 1.5T on a clinical MRI system. (Measurement uncertainty < 1%.)

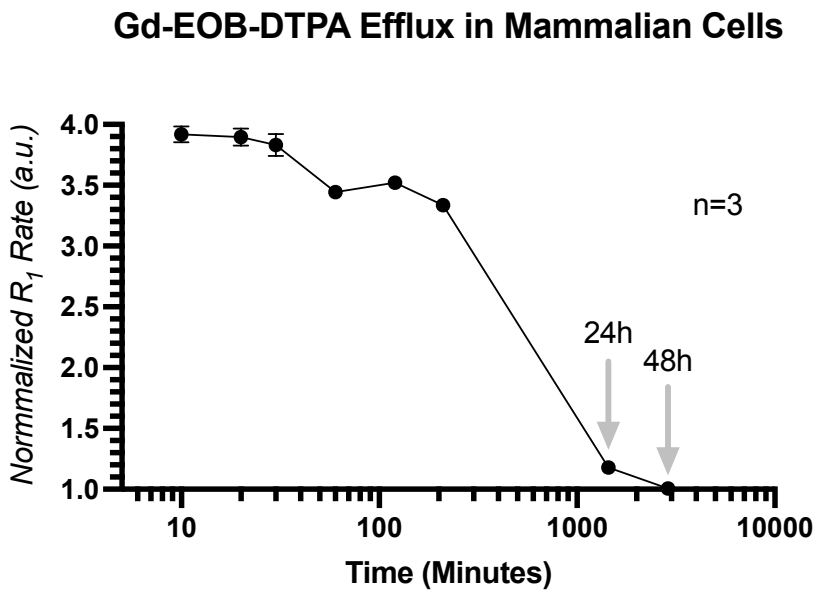

Figure S4. R_1 relaxation rates of Luc-1B3 cells normalized to Luc-CTL cells (a.u.), measured at time, t following 90-minute incubation with 1.6 mM Gd-EOB-TPA and immediate wash with PBS. Measurements were acquired at 37°C, 10 minutes to 48 hours post-incubation. Error bars represent standard deviation. Some error bars are too small to represent on plot.

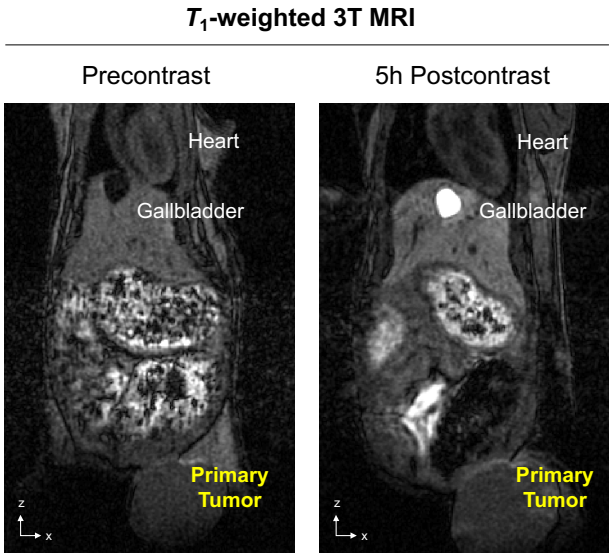

Figure S5. Pre-contrast and post-contrast (1.3-mmol/kg Gd-EOB-DTPA) T_1-weighted images acquired at 3T of a representative Luc-CTL mouse on day 12.

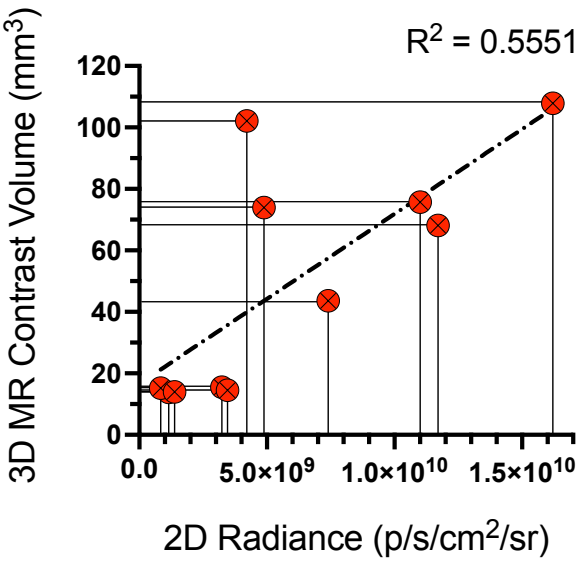

Figure S6. Correlation of 2D Radiance (p/s/cm^2/sr) measured from primary tumors on Day 12 *versus* 3D MRI contrast-enhanced volume of the same primary tumors at the same timepoint.

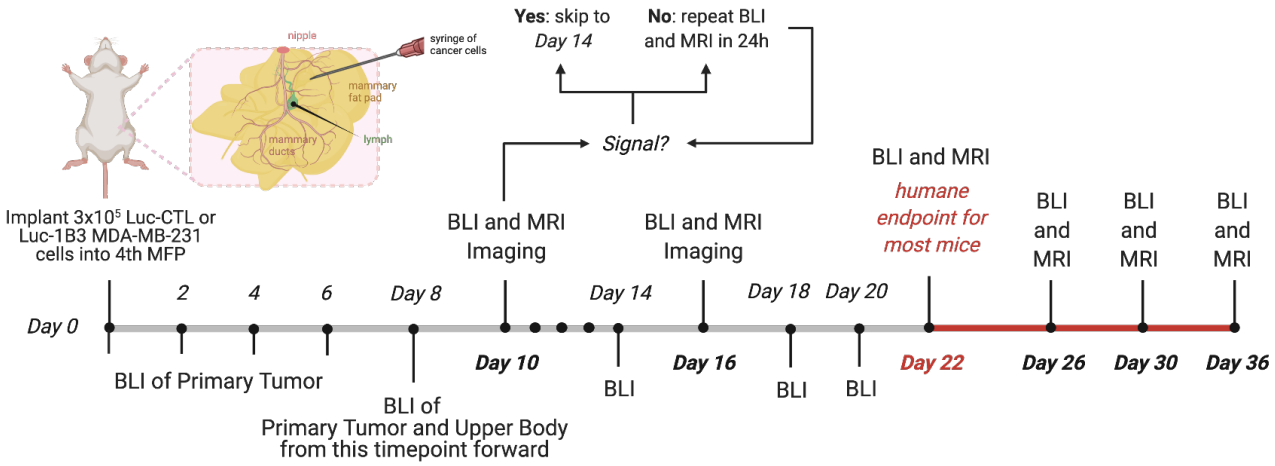

Figure S7. Timeline of metastasis and imaging protocol. Mammary fat pad, MFP. Bioluminescence imaging, BLI. T_1-weighted magnetic resonance imaging at 3T, MRI.

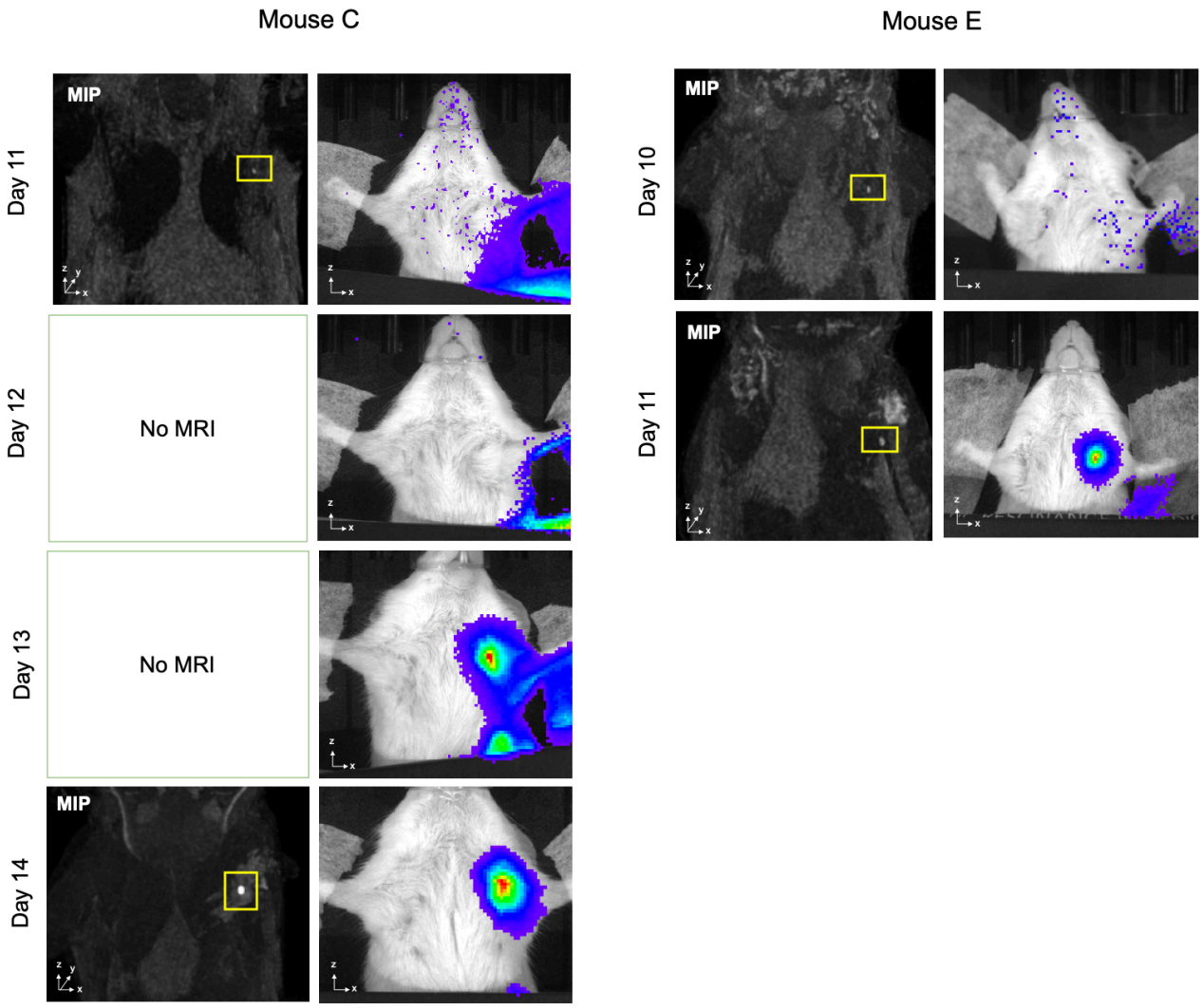

Figure S8. Bioluminescence images (BLI) and post-contrast (1.3 mmol/kg Gd-EOB-DTPA) T_1-weighted images acquired at 3T of two mice, whereby detection of initial metastasis at the ipsilateral axillary lymph node was detected with MRI prior to detection with BLI.